ADVANCED ELECTRONIC MATERIALS Open Access
www.advelectronicmat.de

Improved Polarization-Retention-Endurance in $Hf_{0.5}Zr_{0.5}O_2$ Films by ZrO_2 Capping via Electrostatic Effects

Tingfeng Song, Panagiotis Koutsogiannis, César Magén, José A. Pardo, Florencio Sánchez, and Ignasi Fina**

Ferroelectric hafnia is one of the most promising materials for next generation of non-volatile memory devices. Several strategies have demonstrated to be of interest to improve its functional properties. Interface engineering, realized by the introduction of additional layer in the capacitor structure, is demonstrated as a promising strategy. However, interface layers can have multiple implications, such as changes in the chemistry of the interfaces and an increase of depolarization field, whose effects are difficult to discriminate. The role of HfO_2 and ZrO_2 capping is explored on polarization, retention, endurance, and leakage properties of $Hf_{0.5}Zr_{0.5}O_2$ epitaxial films. In HfO_2 capped films, lower polarization is observed, and endurance and retention are also comparably worse than in ZrO_2 capped films. Complementary under illumination ferroelectric characterization and capacitance measurements indicate a reduction of defects and interface capacitance contribution in ZrO_2 capped films. For both cappings, the interfaces with the $Hf_{0.5}Zr_{0.5}O_2$ layer are shown to be compositionally sharp and the phase of $Hf_{0.5}Zr_{0.5}O_2$ (HZO) grains is replicated on the capping layer, indicating that electrostatic effects prevail and that the use of interface layers with high permittivity, here ZrO_2, is crucial to favor good functional properties.

1. Introduction

Ferroelectric doped HfO_2 is of interest for memory applications due to its CMOS compatibility.[1] In addition, hafnia is also of interest for artificial intelligence engines,[2] energy harvesting applications[3] and nanogenerators, despite its low piezoelectric response.[4] Several strategies are being developed to improve the functional properties of this family of materials.[5] The use of so-called interface layers has demonstrated to be an interesting approach for this purpose. IrO_2[6] and CeO_2[7] layers on top of HZO and Y:HfO_2 (YHO) films, respectively, have shown positive effects on polarization and endurance. It has been claimed that the interface layer provides oxygen[6] and/or stress,[7] which helps to stabilize the ferroelectric orthorhombic phase in the doped HfO_2 film. Other interface layers such as RuO_2,[8] Al_2O_3,[9–11] La_2O_3,[12] or ZrO_2[13] have shown to improve the endurance properties at the expense of a reduced ferroelectric polarization. As it can be seen by relevant functional properties of results of literature summarized in **Table 1**, a variation among results exists. This is probably due to the different oxygen affinity and electrical properties of the characterized interface layers, which have diverse and probably juxtaposed implications. The fact that bare ferroelectric doped HfO_2 films in these studies show very different properties also makes difficult to compare the effect of interface layer among the different reported works. Regarding retention and endurance, the presence of non-ferroelectric phases in single films has been shown to improve endurance[14] at the expense of retention.[15]

T. Song, F. Sánchez, I. Fina
Institut de Ciència de Materials de Barcelona (ICMAB CSIC)
Campus UAB
Bellaterra, Barcelona 08193, Spain
E-mail: fsanchez@icmab.es; ifina@icmab.es

P. Koutsogiannis, C. Magén, J. A. Pardo
Instituto de Nanociencia y Materiales de Aragón (INMA)
CSIC-Universidad de Zaragoza
Zaragoza 50009, Spain

P. Koutsogiannis, C. Magén, J. A. Pardo
Laboratorio de Microscopías Avanzadas (LMA)
Universidad de Zaragoza
Zaragoza 50018, Spain

P. Koutsogiannis, C. Magén
Departamento de Física de la Materia Condensada
Universidad de Zaragoza
Zaragoza 50018, Spain

J. A. Pardo
Departamento de Ciencia y Tecnología de Materiales y Fluidos
Universidad de Zaragoza
Zaragoza 50018, Spain

The ORCID identification number(s) for the author(s) of this article can be found under https://doi.org/10.1002/aelm.202300509

DOI: 10.1002/aelm.202300509

Table 1. Literature and present work values of the effects of interface layers on polarization, endurance, and retention of doped HfO_2 films. Structures are named from top to bottom. *Endurance experiment was performed at 1 MHz in ref. 11, a significantly larger frequency than in the other works. Due to the different experimental conditions used in the literature quantitative comparison of retention can not be done.

Without interface-layer	P_r [μC cm^{-2}]	With interface-layer	P_r [μC cm^{-2}]	Endurance [cycles] [P_r (μC cm^{-2}) @ after indicated cycles]	Retention	Reference
W/HZO/W	21.5	W/HZO/IrO_x	26.5	10^6 [30]	x	[6]
W/YHO/W	1.7	CeO_2/YHO/W	21	$10^{9.5}$ [7]	x	[7]
TiN/HZO/TiN	17	TiN/HZO/RuO_2 or viceversa	25	10^8 [10]	Reported	[8]
TiN/HZO/TiN	27	Al_2O_3/HZO/TiN	21	10^8 [5]	x	[10]
W/HZO/W	12.5	W/Al_2O_3/HZO/W	15.7	near 10^{10} [10]*	x	[11]
TiN/HZO/TiN	18.75	TiN/HZO/La_2O_3	16.25	10^7	Reported	[12]
TiN/$Hf_{0.43}Zr_{0.57}O_2$/SiO_2/Si	1.1	ZrO_2/$Hf_{0.43}Zr_{0.57}O_2$/SiO_2/Si	6.8	3×10^5 [10]	x	[13]
Pt/HZO/LSMO	12	ZrO_2/HZO/LSMO	20	10^{10} [2.5]	Reported	this work

The presence of a non-ferroelectric interface layer at the top might have a similar effect.[16] Besides, retention properties have been scarcely reported in layered systems.[12,17] It is also worth noting that these studies are focused on systems where chemically reactive electrodes, such as TiN, are used, which are known to produce oxygen deficiency at the HfO_2 layer,[18] and that post annealing processes commonly used to stabilize orthorhombic phase can generate blurry interfaces with important chemical interaction. In brief, a comparative study using interface layers showing sharp interfaces and similar oxygen affinity while monitoring polarization-endurance-retention properties is needed.

Beyond the study of interface single layers, nanolaminates based on ZrO_2 and HfO_2 have been studied.[19–21] It has been shown that for increasing the number of layers (at constant total thickness) the system transforms from paraelectric to ferroelectric with important intermixing between layers.[19–21] The enhancement of the ferroelectric polarization is linked to the formation of orthorhombic phase. In this regard, nanolaminate periodicity and annealing temperature have an important impact also on endurance and leakage current.[22,23] Nanolaminates based on Al_2O_3 and ferroelectric doped HfO_2 have demonstrated to be of interest to develop thick (>20 nm) ferroelectric films with sizable polarization,[24,25] of great importance for applications.[26,27]

Epitaxial films, of larger crystalline quality than polycrystalline samples, are of significant interest for understanding characteristics and prototyping devices.[28] In addition, epitaxial films present remarkable distinct functional features respect to the polycrystalline samples, as it is the absence of wake up effect, the rational dependence between coercive field and thickness, and the performance of larger polarization for films below 5 nm.[28,29] However, despite of this interest, interface-layer effects on epitaxial films have been seldomly investigated. Here, we study the impact of ZrO_2 and HfO_2 capping layers of different thickness on $Hf_{0.5}Zr_{0.5}O_2$ epitaxial films. It is shown that the ZrO_2 and HfO_2 cappings have different impact on the ferroelectric polarization, fatigue, and retention of the samples. ZrO_2 capping enhances ferroelectric polarization, endurance, and retention compared with HfO_2 capping. Capacitance dependence on thickness and the effect of interface capacitance has been analyzed. In addition, polarization versus voltage (P–V) loops measured under illumination have been also measured. The results reveal that accumulation of oxygen vacancies most probably occurs for HfO_2 capping.This undesired effect is reduced if ZrO_2 capping is used due to its higher permittivity, which we claim to be at the origin of ZrO_2 capping positive impact on the functional properties. Therefore, changes in the electrostatic boundary conditions imposed by the electric properties of interface layers can result in an improvement of polarization, endurance and retention.

2. Results

Two sets of three epitaxial nominal ≈10 nm-HZO samples capped with HfO_2 or ZrO_2 layers of thicknesses 1, 2, and 3 nm, and one control sample of without capping were prepared on $La_{0.67}Sr_{0.33}MnO_3$ (LSMO) bottom electrode on (001)-oriented $SrTiO_3$ (STO) substrates. The thickness range of the samples under study is above optimal values.[30] This is done to disclose in an easier manner thickness effects from the capping layer effect, due to in the explored range monotonous decrease of polarization with thickness is expected.[30] Pt top contacts were deposited ex-situ. The final structure is sketched in **Figure 1**a. In Figure 1b the P–V loops collected in the HfO_2 capped samples and non-capped HZO sample are shown. 5.5 V was selected as maximum applied voltage to ensure full saturation for all the films; note that the increase of E_c while increasing thickness is not significative and thus the data is comparable. It can be observed that, whereas the film without capping and that with 1 nm capping show similar remanent polarization (P_r = 14 μC cm^{-2} for 0 and 1 nm capping), those with 2 and 3 nm capping show much lower polarization (P_r = 5 μC cm^{-2}). In Figure 1c, the P–V loops collected in the ZrO_2 capped films are shown. Remarkably, it can be observed that irrespective of the ZrO_2 capping thickness the polarization remains nearly constant and as large as 20 μC cm^{-2} with loops of the 1 and 2 nm capped films almost overlapping. From data included in Figure 1b,c, it can be concluded that the ZrO_2 capping results in an enhancement of polarization with respect to pure HZO films, contrary to HfO_2 capping. Same trend is observed for values obtained using PUND method (Figure 1d,e). In Figure 1f, P_r values obtained on the different samples as a function of capping thickness are summarized. The larger polarization for any capping thickness in the ZrO_2 case compared to that

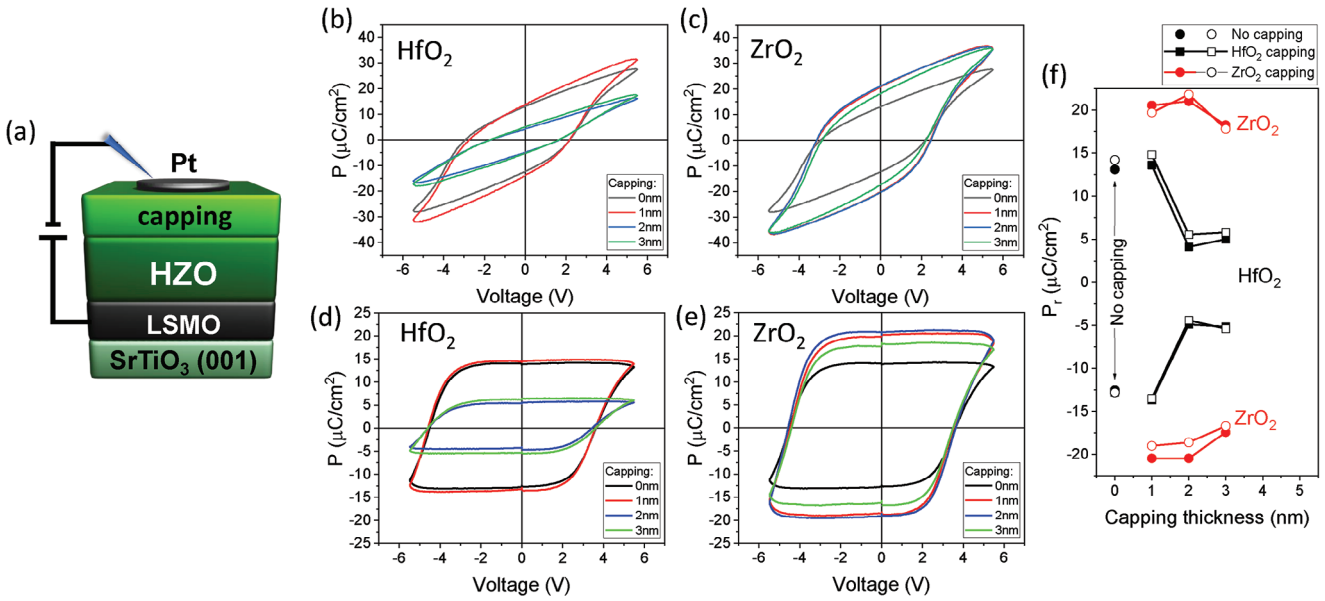

Figure 1. a) Sketch of the HZO devices. b,c) *P–V* loops of the HfO_2 and ZrO_2 capped films, respectively, with the indicated capping thickness. d,e) *P–V* PUND loops of the HfO_2 and ZrO_2 capped films, respectively, with the indicated capping thickness. f) Summary of the P_r values as a function of the capping thickness. Black round circles correspond to the non-capped film of the present work. Solid symbols correspond the P_r values extracted from the loops shown in panels (b,c). Empty symbols correspond the P_r values extracted from the PUND loops shown in panels (d,e).

of HfO_2 can be clearly inferred. Note that the values of polarization in the explored thickness range are greater than the reported ones in single-layer epitaxial HZO films.[30]

Figure 2a,b shows XRD 2θ–χ maps of the non-capped film and the films capped with HfO_2 and ZrO_2 measured with a 2D detector. The brighter spots correspond to the overlapping reflections of the STO substrate and the LSMO electrode. HZO spots appear at ≈28.3°, ≈30°, and ≈34.4°, which correspond to the position of the monoclinic (−111), orthorhombic (111) and monoclinic (002) reflections, respectively. Monoclinic (002) reflection is present in all the samples, while the monoclinic (−111) reflection is suppressed in the ZrO_2 capped films. The low intensity circular spot at similar position (≈29°) is a Laue oscillation of the orthorhombic (111) reflection (Figure S1, Supporting Information). Note also that the orthorhombic (111) reflection overlaps with the tetragonal (101) peak and that the monoclinic (002) reflection can be overlapped with both the (002) orthorhombic and the (002) tetragonal ones. It is apparent that the monoclinic reflections expand along χ, whereas the orthorhombic one does not, indicating the larger mosaicity of the monoclinic phase.

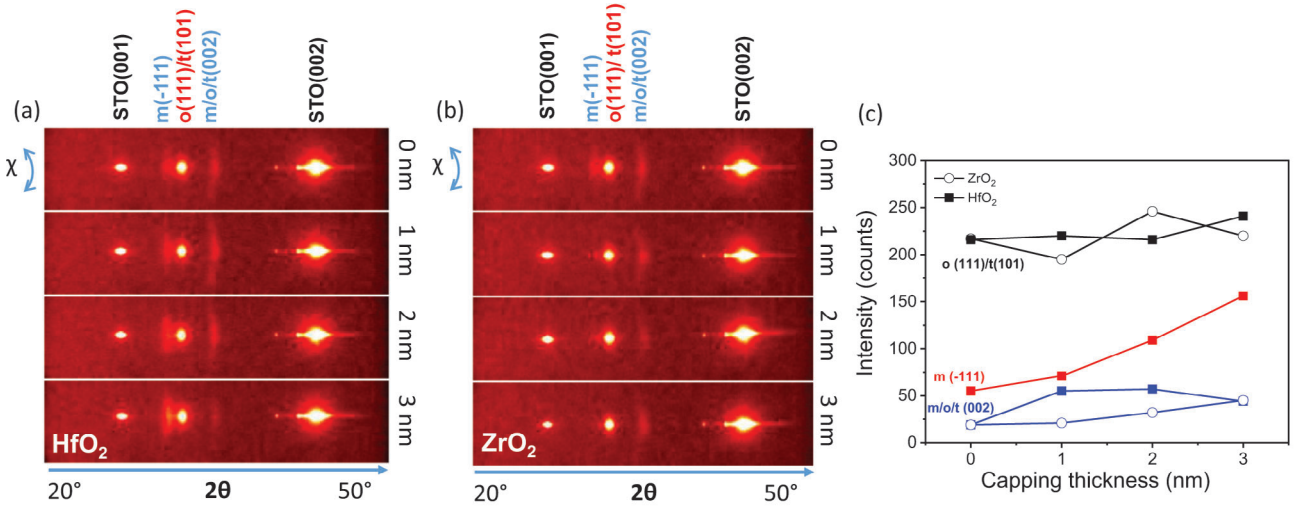

Figure 2. a,b) XRD 2θ–χ maps of the non-capped film and films capped with HfO_2 and ZrO_2, respectively. c) Intensity (after background subtraction) of the monoclinic (−111) and monoclinic/orthorhombic/tetragonal (002) and orthorhombic (111)/ tetragonal (101) reflections as a function of capping thickness (see integrated 2θ scans in Figure S2, Supporting Information).

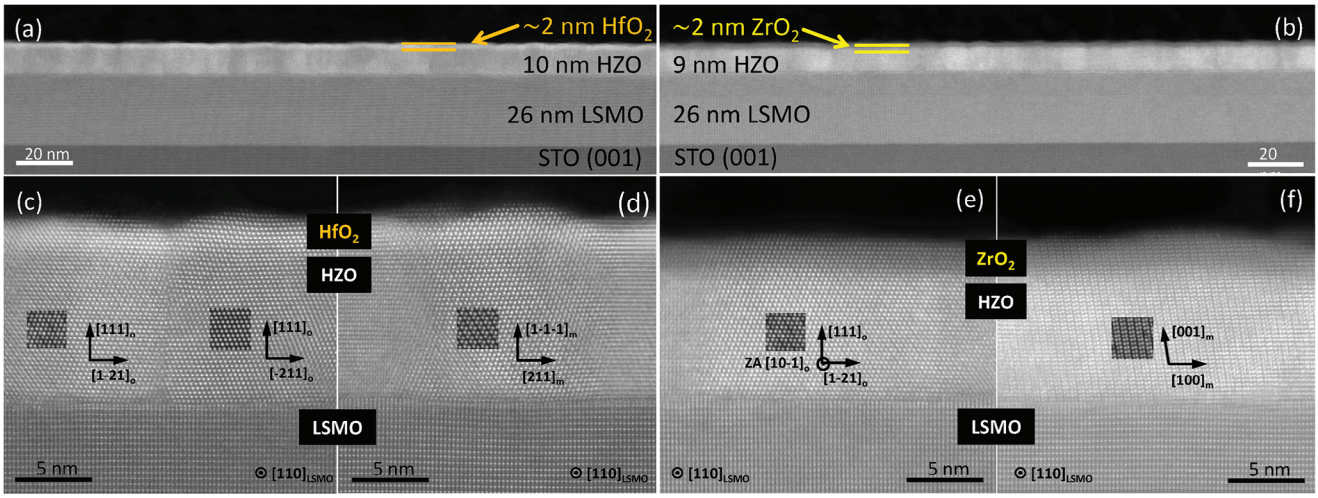

Figure 3. Low magnification HAADF-STEM images of the 2 nm-thick a) HfO_2 and b) ZrO_2 capped HZO films. Representative orthorhombic grains with their corresponding epitaxy relations of the 2-nm-thick c) HfO_2 and e) ZrO_2 capped HZO films. Representative monoclinic grains with their corresponding epitaxy relations and image simulations of the structure of the 2 nm-thick d) HfO_2 and f) ZrO_2 capped HZO films. Zone axis corresponds to the [110] direction of LSMO.

Considering this mosaicity, 2θ scans were obtained by integrating in $\chi = \pm 10^{o}$ (Figure S2, Supporting Information). The integrated intensity of the monoclinic (−111) (except for ZrO_2 capped films), monoclinic (002), and orthorhombic (111) reflections is plotted as a function of the capping thickness in Figure 2c. It can be observed that in both sets of samples the orthorhombic peak intensity is approximately constant. However, the peak corresponding to monoclinic (−111) phase is present and increases with HfO_2 capping thickness. The intensity of the monoclinic (002) reflection is low in all samples and shows no evident dependence on thickness. Thus, the main difference between the two sets of samples is the presence of monoclinic (−111) reflection in HfO_2 capped films, which increases its intensity with the HfO_2 capping thickness.

In **Figure 3**, we evaluate the local microstructure and the interface sharpness of the films, where HAADF-STEM cross-sectional images of 2 nm-thick HfO_2 and ZrO_2 capped films are shown. Low magnification images (Figure 3a,b) show thickness values ≈10 and 9 nm for the HZO layer and ≈2 nm for the HfO_2 and ZrO_2 capping, respectively, in good agreement with thicknesses obtained from Laue oscillations fitting (Figure S1, Supporting Information). The different thickness of the samples is a result of the slightly different growth rate due to experimental variability during the growth of the films on different processes without relevant impact on structural properties. The LSMO bottom electrode and STO substrate are also shown. Figure 3c,e show representative examples of HZO orthorhombic grains, evidencing that the HfO_2 or ZrO_2 capping layer adopts its same orthorhombic structure and orientation. Figure 3d shows one monoclinic (−111) grain for the HfO_2-capped sample. In this case HfO_2 capping also replicates the crystal structure of the HZO layer. Similarly, the monoclinic (001) grain shown in Figure 3f shows uniform structure in the HZO layer and the ZrO_2-capping. An equivalent conclusion can be deduced from Supporting Information Figure S3 (Supporting Information), in which monoclinic and orthorhombic grains with different orientation in the HZO layer also show replicated crystal structure in their HfO_2 and ZrO_2 cappings. Therefore, there is crystalline coherence between the HZO layer and the capping.

Figure 4a,b shows maps obtained by data interpolation of endurance as a function of cycling voltage and capping thickness for HfO_2 and ZrO_2 capping, respectively. Endurance graphs of all the samples are presented in Figure S4 (Supporting Information). Endurance values in Figure 4a,b correspond to the number of cycles up to that P_r is above 2.5 μC cm^{-2}. For the 1 nm-thick HfO_2 capping, it can be observed that endurance is up to 10^{10} cycles, but not for the other capping thicknesses and the non-capped HZO film. This high endurance is larger than the values reported in capped structures of polycrystalline films (Table 1).[6–8,10,12] The endurance map for ZrO_2 capping shows a similar result. At higher and lower than the optimal voltage values fatigue is larger due to faster degradation of device and to overall lower switchable polarization, respectively. Note that all the films show severe fatigue during the first cycles (Figure S4, Supporting Information). This severe fatigue can be ascribed to field induce phase transition during cycling,[31] or defects redistribution. However, the relevant role of the capping layer indicates that defects redistribution is likely at the origin as discussed below, due to similar behavior would be expected in presence of phase transition while comparing both sets of samples. Despite of that, all samples show $2{\cdot}P_r > 2.5$ μC cm^{-2} after 10^7 cycles indicating their good endurance properties compared with the reported endurance of polycrystalline bilayer systems (Table 1), in addition of the absence of wake-up effect (Supporting information Figure S4, Supporting Information), as commonly found in epitaxial films.[28] The polarization evaluated after 10^6 cycles as a function of cycling voltage and capping thickness is shown in Figure 4c,d. It can be observed that the range (voltage and capping layer thickness) where polarization in ZrO_2 capping is higher than 4 μC cm^{-2} is substantially wider compared with the case of HfO_2 capping. In Figure 4e, loops after 10^6 cycles for 1 nm-thick capping of HfO_2 and ZrO_2 are shown, as an example to visualize the larger

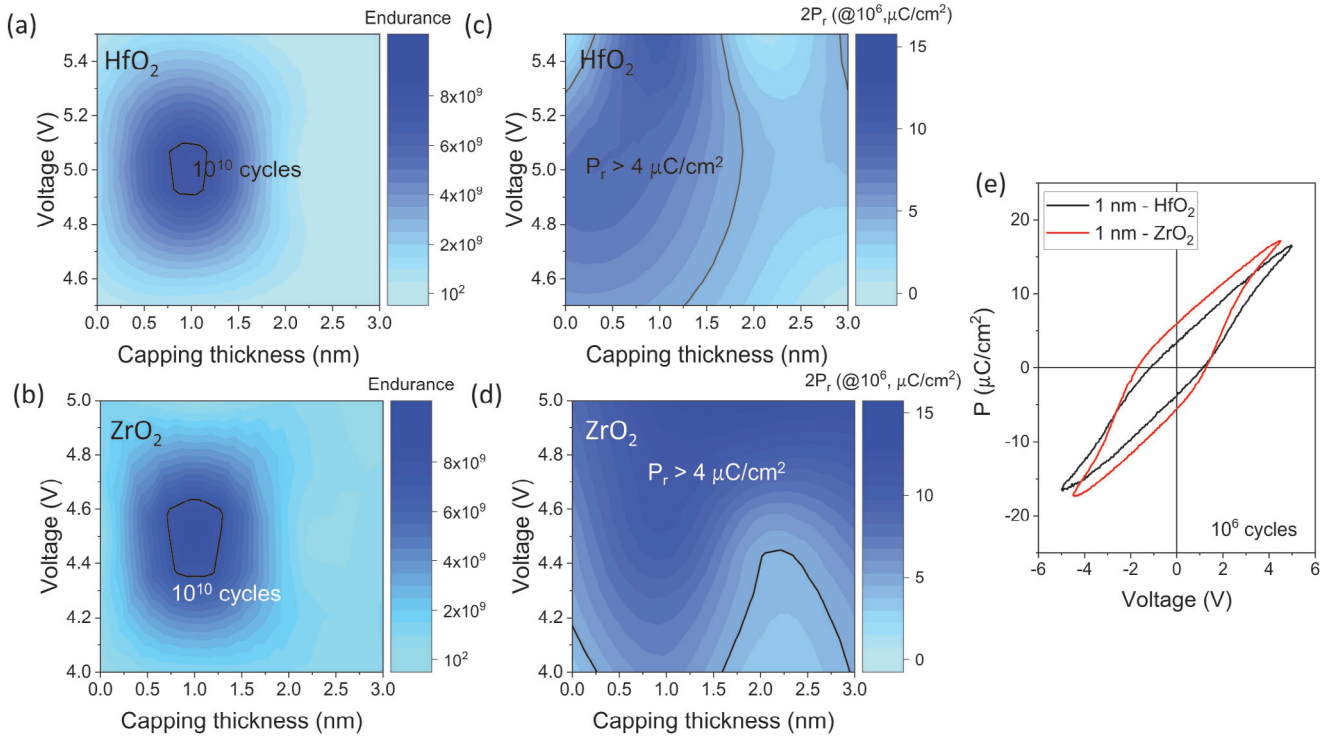

Figure 4. a,b) Map of HZO endurance as a function of cycling voltage and capping thickness for HfO_2 and ZrO_2 capping, respectively. c,d) Map of polarization evaluated after 10^6 cycles as a function of cycling voltage and capping thickness for HfO_2 and ZrO_2, respectively. Maps are done by interpolation of data included inFigure S4 (Supporting Information). e) *P–V* loops after 10^6 cycles for 1 nm HfO_2 and ZrO_2 capped films. Note that loops shown in (e) were measured and cycled at the optimal cycling voltage for each capping layer, 5 and 4.5 V for HfO_2 and ZrO_2 capping, respectively.

polarization of ZrO_2 capped films after cycling. Therefore, the presence of ZrO_2 capping enhances also endurance.

In **Figure 5**a,b, the retention evaluated for representative 1- and 2 nm-thick HfO_2 and ZrO_2 capping is shown. The retention data for all the samples is presented in Supporting Information Figure S5 (Supporting Information). Extrapolated polarization at 10 year is ≈12 μC cm^{-2} for ZrO_2 capped layers, much above non-capped and HfO_2 capped samples (Figure S5, Supporting Information). The used maximum delay time in the retention experiments is lower than that reported for RuO_2[8] and La_2O_3[12] capped polycrystalline films, hindering direct comparison. In any case, the retention for the HfO_2 capping is lower compared with the ZrO_2, suggesting that depolarization fields play a larger role in samples with HfO_2 capping. A better performance for ZrO_2 capping is also observed in the leakage curves of representative 2 nm-thick HfO_2 and ZrO_2 capped films, plotted in Figure 5c. Leakage curves for all the samples are displayed in Supporting Information Figure S6 (Supporting Information). Leakage in the pristine state is similar in both samples. However, after 10^6 cycles (at 5 V and 100 kHz) the leakage evaluated at 1 V for HfO_2 capping is near two orders of magnitude larger than for ZrO_2 capping. This indicates a larger presence of defects in HfO_2 capped films. *P–V* loops of the same samples in dark and under illumination with light of 405 nm wavelength are plotted in Figure 5d. It can be observed that the 2 nm-thick HfO_2 capped films show a reduction of the polarization under illumination. Being the bandgap of HfO_2 much larger (≈ 5.8 eV)[32–34] than the used photon energy (3.06 eV), the observed photoresponse indicates a larger presence of defects, likely oxygen vacancies, in HfO_2 capped films.[35,36]

3. Discussion

In brief, we have found that a thin ZrO_2 capping layer enhances polarization, retention and endurance respect to the HfO_2 capping. First, it might be argued that it is a thickness effect. It is usual in polycrystalline and epitaxial films that the highest polarization occurs at certain thickness. However, in the explored equivalent thickness range one should expect a decrease of polarization with thickness[30,37] instead of an increase, disregarding the thickness effect at the origin of the polarization enhancement by ZrO_2 capping. If we consider the total thickness of the film, which vary while comparing HfO_2 and ZrO_2 capped films (see Figure S1, Supporting Information) a similar scenario holds. Second, it is known that HZO polarization strongly depends on the Hf/Zr ratio. Larger Hf or Zr content in polycrystalline films results in a reduction of the P_r due to increased content of monoclinic or tetragonal phase, respectively.[38] In epitaxial films the variation of Hf/Zr ratio has a smoothed impact on polarization.[39] Therefore, the mere presence of larger amount of Zr in ZrO_2 capped samples compared with the HfO_2 ones, might lower the formation energy for the orthorhombic phase, increasing its relative amount and therefore positively impacting on the polarization. However, considering capped films as single-layers, the overall compositions shift to Zr (Hf) rich for ZrO_2 (HfO_2) capping in the x = 0.4 to 0.6 range of $Hf_xZr_{1-x}O_2$. The increase

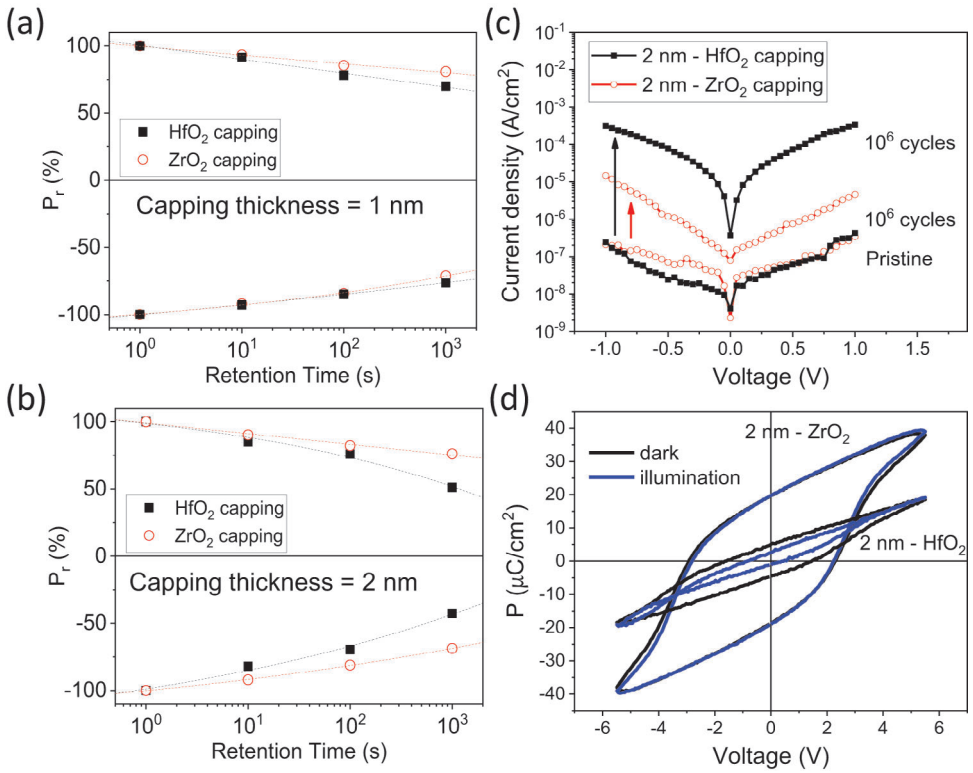

Figure 5. a,b) Retention at room temperature using opposite state pulse train of 1 and 2 nm capped HZO films, respectively. Dash lines are guide for the eye. c) Leakage current versus voltage of 2 nm capped films in pristine state and after 10^6 cycles at 100 kHz. d) *P–V* loops of 2 nm capped HZO films in dark and under illumination.

of monoclinic phase for HfO_2 capping follows the trend reported for epitaxial single layers with different Zr/Hf ratio.[39] However, the 50 % increase of P_r found here for ZrO_2 capping largely overpasses the minute increase that one would expect for $Hf_{0.4}Zr_{0.6}O_2$ as extrapolated from reported data.[39]

A plausible third scenario to account for the positive impact of ZrO_2 capping in all the measured functional properties is described as follows. As data below indicate, HfO_2 layers show lower permittivity than ZrO_2 layer ones. The lower HfO_2 permittivity results in a larger depolarization field. These depolarization fields might have in-plane and out-of-plane contributions.[40] Electric imprint field is toward LSMO, thus polarization is downward during the growth and/or cooling of the film and concomitant orthorhombic phase formation. Therefore, the larger depolarization field can favor an accumulation of oxygen vacancies at the HZO/HfO_2 top interface (**Figure 6**a), as reported at the interfaces of polycrystalline films with other capping oxides.[8] As a result, larger interface capacitance should be observed in HZO films with HfO_2 capping. Note that after growth, oxygen vacancies are likely not charged, as revealed by the small difference on the E_{imp} between HfO_2 and ZrO_2 capped films (Figure 1).

Indeed, in Figure 6c, the reciprocal capacitance as a function of capping thickness is shown. Note that in this case the reciprocal capacitance can be computed through the following relation for three capacitors in series:

$$\frac{1}{C_{total}} = \frac{1}{C_i} + \frac{1}{C_{HZO}} + \frac{1}{C_{capping}} = \frac{1}{C_i} + \frac{t_{HZO}}{\epsilon_0 \epsilon_{HZO} S} + \frac{t_{capping}}{\epsilon_0 \epsilon_{capping} S} \quad (1)$$

where C_i, C_{HZO} and $C_{capping}$ are the interface capacitance, the HZO capacitance and the capping layer capacitance, respectively. S is the electrode area, t_{HZO} and $t_{capping}$ account for the thickness of the HZO layer and capping layer, respectively. Thus, the intercept of the reciprocal capacitance shown in Figure 6c should be $\frac{1}{C_i} + \frac{1}{C_{HZO}}$. In the case of the ZrO_2 set of samples the intercept is near the $\frac{1}{C_{HZO}}$ (triangle in Figure 6c), which is estimated from the capacitance measured in the non-capped film. This indicates the small additional contribution of C_i in the ZrO_2 set. Instead, for the HfO_2 set of samples the intercept is larger, indicating that there is a sizeable contribution of C_i, meaning a thicker and/or lower-permittivity dead layer. In Figure 6d, the $\frac{1}{C_i} + \frac{1}{C_{HZO}}$ term (right axis) for both sets is plotted and compared with the $\frac{1}{C_{HZO}}$ from the non-capped film. It can be more clearly appreciated that the $\frac{1}{C_i} + \frac{1}{C_{HZO}}$ term is similar to $\frac{1}{C_{HZO}}$ for ZrO_2 but not for HfO_2. In epitaxial films ϵ_r varies ≈5 per 10 nm in the explored thickness range due to the orthorhombic phase ratio change, as reported elsewhere.[29] This possible variation has been added as error bar in Figure 6c,d and it can be observed that its effect should be negligible. Therefore, the different slope of the two sets of samples account for the different ϵ_r of the capping layers (see Equation 1). Using Equation 1, ϵ_r is extracted and plotted in figure 6d (left axis). It can be observed that ϵ_r is significantly smaller for HfO_2 capping, as it is also reported in HfO_2 epitaxial films in comparison to doped ones.[41] Besides, the presence of larger leakage current, photoresponse and presence of interface capacitance in the

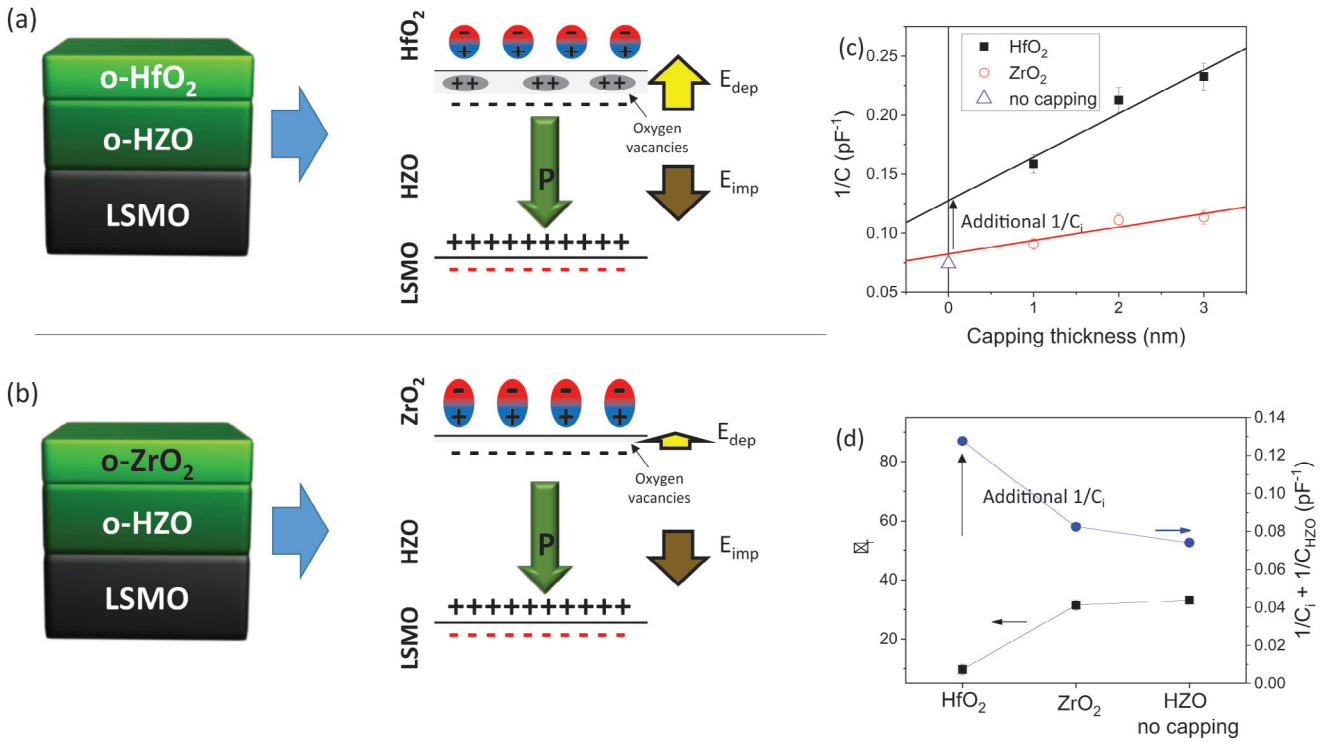

Figure 6. a,b) Sketch of the different accumulation of oxygen vacancies depending on the capping. c) Reciprocal of capacitance as a function of the capping thickness. d) Permittivity extracted from the slope of the straight-line fits shown in panel (c) in left axis. $\frac{1}{C_i} + \frac{1}{C_{HZO}}$ term extracted from the intercept point of the straight-line fits shown in panel (c) in right axis. Permittivity and reciprocal capacitance of the non-capped HZO sample are also included.

HfO_2 capped films shown in Figure 5c, indicate the large presence of oxygen deficiency at the interface. During cycling these defects are probably redistributed causing severe fatigue as observed (Figure S4, Supporting Information).Contrary to previous results on polycrystalline films,[42,43] the presence of larger number of defects at the interface, does not produce here wake-up effects (Figure S4, Supporting Information), indicating the positive role of sharp interfaces of epitaxial films. Therefore, the presence of a higher permittivity capping has an ultimate positive impact on the main functional properties: polarization and reliability and interface-layer with high permittivity would be mandatory to avoid large amount of defects. In addition, orthorhombic phase has been also stabilized in ZrO_2 films enabling polarization values up to 50 μC cm^{-2}.[44,45] Thus additional positive contribution of this largely polarizable phase can further promote the good performance of ZrO_2 capped samples. Alternatively, the opposite band bending expected due to the different electron affinity of HfO_2 and ZrO_2,[46] can also result in a similar effect, i.e., accumulation of oxygen defects in one case and not in the other.

4. Conclusion

It has been shown that ZrO_2 capping results in higher polarization-endurance-retention than HfO_2 capping. Leakage and photoferroelectric response experiments indicate that the number of defects is larger in HfO_2 capped films. Capacitance characterization shows that interface capacitance contribution is also more important in HfO_2 capped films than in ZrO_2 ones, which indicates that defects are probably accumulated at HZO/HfO_2 interface. We suggest that the lower permittivity of HfO_2 causes a larger contribution of the interface capacitance, increasing also the depolarization field that generates accumulation of defects at the interface, impacting negatively on functional properties. The absence of evident Hf/Zr intermixing at the interfaces excludes that interface chemistry plays a relevant role and that electrostatic effects prevail. Therefore, we have further demonstrated the dominant role of the dead layer presence and established a strategy, the use of high permittivity capping, to reduce it, resulting in a positive effect on relevant functional properties, such as polarization-endurance-retention. Despite integration of the proposed approximation in devices would require further relevant characterization, using higher frequency endurance tests during greater number of cycles and retention experiments in harsh environments during longer delay times, and further materials optimization by different doping and/or thickness selection, the strategy presented here, represents a solid base for further progress.

5. Experimental Section

Bottom LSMO electrodes, ferroelectric HZO films, and HfO_2 and ZrO_2 capping layers were grown on (001)-oriented STO substrates in a

single process by pulsed laser deposition using a KrF excimer laser (248 nm wavelength). The LSMO bottom electrodes, with a thickness $t \approx 25$ nm, were grown at a substrate temperature of $T_S = 700$ °C and oxygen pressure $P_{O2} = 0.1$ mbar.[47] HZO, HfO_2, and ZrO_2 layers were grown at 800 °C and $P_{O2} = 0.1$ mbar, as reported elsewhere.[48] The substrate temperature was measured using a thermocouple inserted in the middle of the heater block. Structural characterization was performed by X-ray diffraction (XRD) using Cu Kα radiation. Atomic-scale structural analysis of selected films was performed by scanning transmission electron microscopy (STEM) in high-angle annular dark field (HAADF) imaging mode. A Thermo Fisher Titan 60–300 microscope equipped with a high brightness Schottky field emission gun and a CETCOR probe-corrector (CEOS Gmbh) was operated at 300 kV to provide a probe size below 0.1 nm. Cross-sectional lamellas of the specimens, cut along (110) and (100) planes of the STO substrate were prepared by Focused Ion Beam milling in a Thermo Fisher Helios 650 Nanolab. STEM image simulations were carried out with the Dr. Probe software package.[49] Platinum top electrodes for electrical characterization, 20 nm-thick and 20 µm in diameter, were grown by dc magnetron sputtering through stencil masks. Ferroelectric characterization was done using a TFAnalyzer2000 (AixAcct Gmbh) platform. Ferroelectric polarization loops were measured at 1 kHz using the dynamic leakage current compensation (DLCC) procedure at room temperature with the bottom electrode being grounded.[50] Endurance was studied by cycling the sample at 100 kHz using bipolar square pulses of the indicated amplitude and measuring polarization loops at 1 kHz. Retention was characterized at room temperature by prepolarizing the sample with a pulse 5.5 V amplitude and measuring the polarization state by Positive-Up-Negative-Down (PUND) method using the opposite state pulse train.[8,41] Leakage was measured with 1 s integration time for each point. Capacitance (C) loops were measured by using an impedance analyzer (HP4192LF, Agilent Co.) operated with an excitation voltage (V_{AC}) of 300 mV at 100 kHz. 300 mV had been selected due to it is the largest one with no contribution of ferroelectric switching or domain wall motion contribution (see Supporting Information Figure S7, Supporting Information). Under illumination experiments have been done by direct illumination of the characterized capacitor with light of 405 nm wavelength and with a power density of ≈200 mW cm^{-2}. Further details on the set-up are described elsewhere.[51] Note that at the used wavelength transparency of Pt electrodes is ≈14%, ensuring important amount of light reaching the interface.[52,53]

Supporting Information

Supporting Information is available from the Wiley Online Library or from the author.

Acknowledgements

Financial support from the Spanish Ministry of Science and Innovation (MCIN/AEI/ 10.13039/501100011033), through the Severo Ochoa FUNFUTURE (CEX2019-000917-S), PID2020-112548RB-I00, PID2020-112914RB-I00 and PID2019-107727RB-I00 projects and from Generalitat de Catalunya (2021 SGR 00804) are acknowledged. The authors also acknowledge project TED2021-130453B-C21, funded by MCIN/AEI/10.13039/501100011033 and European Union NextGeneration EU/PRTR, and EU Horizon 2020 programme under the Marie Skłodowska-Curie grant agreement No. 861153 MANIC. T.S. is financially supported by China Scholarship Council (CSC) with No. 201807000104.

Conflict of Interest

The authors declare no conflict of interest.

Data Availability Statement

The data that support the findings of this study are available from the corresponding author upon reasonable request.

Keywords

endurance, epitaxial HfO_2, ferroelectric hafnia, HZO, interface layer, nanolaminates, retention

Received: July 31, 2023
Revised: November 21, 2023
Published online:

[1] T. Mikolajick, M. H. Park, L. Begon-Lours, S. Slesazeck, *Adv. Mater.* **2023**, *35*, 2206042.
[2] A. Keshavarzi, K. Ni, W. V. D. Hoek, S. Datta, A. Raychowdhury, *IEEE Micro* **2020**, *40*, 33.
[3] F. Ali, T. Ali, D. Lehninger, A. Sünbül, A. Viegas, R. Sachdeva, A. Abbas, M. Czernohorsky, K. Seidel, *Adv. Funct. Mater.* **2022**, *32*, 2201737.
[4] T. Tharpe, E. Hershkovitz, F. Hakim, H. Kim, R. Tabrizian, *Nat. Electron.* **2023**, *6*, 599.
[5] K. Yang, S. H. Kim, H. W. Jeong, D. H. Lee, G. H. Park, Y. Lee, M. H. Park, *Chem. Mater.* **2023**, *35*, 2219.
[6] M. Yadav, A. Kashir, S. Oh, R. D. Nikam, H. Kim, H. Jang, H. Hwang, *Nanotechnology* **2022**, *33*, 085206.
[7] K. Mizutani, T. Hoshii, H. Wakabayashi, K. Tsutsui, E. Y. Chang, K. Kakushima, *Jpn. J. Appl. Phys.* **2022**, *61*, 021006.
[8] Y. Goh, S. H. Cho, S.-H. K. Park, S. Jeon, *Nanoscale* **2020**, *12*, 9024.
[9] J. Wang, D. Wang, Q. Li, A. Zhang, D. Gao, M. Guo, J. Feng, Z. Fan, D. Chen, M. Qin, M. Zeng, X. Gao, G. Zhou, X. Lu, J. M. Liu, *IEEE Electron Device Lett.* **2019**, *40*, 1937.
[10] H. A. Hsain, Y. Lee, S. Lancaster, P. D. Lomenzo, B. Xu, T. Mikolajick, U. Schroeder, G. N. Parsons, J. L. Jones, *Nanotechnology* **2023**, *34*, 125703.
[11] B. Liu, Y. Cao, W. Zhang, Y. Li, *Appl. Phys. Lett.* **2021**, *119*, 172902.
[12] F. Mehmood, R. Alcala, P. Vishnumurthy, B. Xu, R. Sachdeva, T. Mikolajick, U. Schroeder, *Adv. Mater. Interfaces* **2023**, *10*, 2202151.
[13] T. Onaya, T. Nabatame, M. Inoue, T. Sawada, H. Ota, Y. Morita, *APL Mater.* **2022**, *10*, 051110.
[14] T. Song, S. Estandía, H. Tan, N. Dix, J. Gàzquez, I. Fina, F. Sánchez, *Adv. Electron. Mater.* **2022**, *8*, 2100420.
[15] F. Mehmood, M. Hoffmann, P. D. Lomenzo, C. Richter, M. Materano, T. Mikolajick, U. Schroeder, *Adv. Mater. Interfaces* **2019**, *6*, 1901180.
[16] N. Gong, T. P. Ma, *IEEE Electron Device Lett.* **2016**, *37*, 1123.
[17] R. Alcala, F. Mehmood, P. Vishnumurthy, T. Mittmann, T. Mikolajick, U. Schroeder, in *2022 IEEE International Memory Workshop (IMW)*, IEEE, Piscataway. NJ **2022**.
[18] W. Hamouda, F. Mehmood, T. Mikolajick, U. Schroeder, T. O. Mentes, A. Locatelli, N. Barrett, *Appl. Phys. Lett.* **2022**, *120*, 202902.
[19] S. L. Weeks, A. Pal, V. K. Narasimhan, K. A. Littau, T. Chiang, *ACS Appl. Mater. Interf.* **2017**, *9*, 13440.
[20] Y. K. Liang, W. L. Li, Y. J. Wang, L. C. Peng, C. C. Lu, H. Y. Huang, S. H. Yeong, Y. M. Lin, Y. H. Chu, E. Y. Chang, C. H. Lin, *IEEE Electron Device Lett.* **2022**, *43*, 1451.
[21] N. Bai, K.-H. Xue, J. Huang, J.-H. Yuan, W. Wang, G.-Q. Mao, L. Zou, S. Yang, H. Lu, H. Sun, X. Miao, *Adv. Electron. Mater.* **2023**, *9*, 2200737.
[22] D. Lehninger, A. Sünbül, R. Olivo, T. Kämpfe, K. Seidel, M. Lederer, in *2023 IEEE International Memory Workshop (IMW)*, IEEE, Piscataway, NJ **2023**.
[23] D. Lehninger, A. Prabhu, A. Sünbül, T. Ali, F. Schöne, T. Kämpfe, K. Biedermann, L. Roy, K. Seidel, M. Lederer, L. M. Eng, *Adv. Phys. Res.* **2023**, *2*, 2200108.
[24] H. J. Kim, M. H. Park, Y. J. Kim, Y. H. Lee, W. Jeon, T. Gwon, T. Moon, K. D. Kim, C. S. Hwang, *Appl. Phys. Lett.* **2014**, *105*, 192903.
[25] S. Riedel, P. Polakowski, J. Müller, *AIP Adv.* **2016**, *6*, 095123.

[26] S. Kirbach, K. Kühnel, W. Weinreich, in *Piezoelectric Hafnium Oxide Thin Films for Energy-Harvesting Applications, 2018 IEEE 18th International Conference on Nanotechnology*, IEEE, Piscataway, NJ **2018**.
[27] X.-Q. Zheng, T. Tharpe, S. M. Enamul Hoque Yousuf, N. G. Rudawski, P. X. L. Feng, R. Tabrizian, *ACS Appl. Mater. Interf.* **2022**, *14*, 36807.
[28] I. Fina, F. Sanchez, *ACS Appl. Electron. Mater.* **2021**, *3*, 1530.
[29] J. Lyu, T. Song, I. Fina, F. Sanchez, *Nanoscale* **2020**, *12*, 11280.
[30] J. Lyu, I. Fina, R. Solanas, J. Fontcuberta, F. Sánchez, *ACS Appl. Electron. Mater.* **2019**, *1*, 220.
[31] T. S. Böscke, S. Teichert, D. Bräuhaus, J. Müller, U. Schröder, U. Böttger, T. Mikolajick, *Appl. Phys. Lett.* **2011**, *99*, 112904.
[32] J. Robertson, *J. Vac. Sci. Technol.* **2000**, *18*, 1785.
[33] H. Kato, T. Nango, T. Miyagawa, T. Katagiri, K. S. Seol, Y. Ohki, *J. Appl. Phys.* **2002**, *92*, 1106.
[34] F. L. Martínez, M. Toledano-Luque, J. J. Gandía, J. Cárabe, W. Bohne, J. Röhrich, E. Strub, I. Mártil, *J. Phys. D: Appl. Phys.* **2007**, *40*, 5256.
[35] M. Grossmann, O. Lohse, D. Bolten, U. Boettger, T. Schneller, R. Waser, *J. Appl. Phys.* **2002**, *92*, 2680.
[36] M. Grossmann, O. Lohse, D. Bolten, U. Boettger, R. Waser, *J. Appl. Phys.* **2002**, *92*, 2688.
[37] T. Song, R. Bachelet, G. Saint-Girons, N. Dix, I. Fina, F. Sánchez, *J. Mater. Chem. C* **2021**, *9*, 12224.
[38] J. Müller, T. S. Böscke, U. Schröder, S. Mueller, D. Bräuhaus, U. Böttger, L. Frey, T. Mikolajick, *Nano Lett.* **2012**, *12*, 4318.
[39] T. Song, H. Tan, N. Dix, R. Moalla, J. Lyu, G. Saint-Girons, R. Bachelet, F. Sánchez, I. Fina, *ACS Appl. Electron. Mater.* **2021**, *3*, 2106.
[40] M. Pesic, F. P. G. Fengler, L. Larcher, A. Padovani, T. Schenk, E. D. Grimley, X. Sang, J. M. Lebeau, S. Slesazeck, U. Schroeder, T. Mikolajick, *Adv. Funct. Mater.* **2016**, *26*, 4601.
[41] T. Song, H. Tan, R. Bachelet, G. Saint-Girons, I. Fina, F. Sánchez, *ACS Appl. Electron. Mater.* **2021**, *3*, 4809.
[42] D. Zhou, J. Xu, Q. Li, Y. Guan, F. Cao, X. Dong, J. Müller, T. Schenk, U. Schröder, *Appl. Phys. Lett.* **2013**, *103*, 192904.
[43] H. J. Kim, M. H. Park, Y. J. Kim, Y. H. Lee, T. Moon, K. D. Kim, S. D. Hyun, C. S. Hwang, *Nanoscale* **2016**, *8*, 1383.
[44] Y. Cao, W. Zhang, Y. Li, *Nanoscale* **2023**, *15*, 1392.
[45] K.-W. Huang, S.-H. Yi, Y.-S. Jiang, W.-C. Kao, Y.-T. Yin, D. Beck, V. Korolkov, R. Proksch, J. Shieh, M.-J. Chen, *Acta Mater.* **2021**, *205*, 116536.
[46] W. Zheng, K. H. Bowen, J. Li, I. Dąbkowska, M. Gutowski, *J. Phys. Chem. A* **2005**, *109*, 11521.
[47] J. Lyu, I. Fina, R. Solanas, J. Fontcuberta, F. Sánchez, *Appl. Phys. Lett.* **2018**, *113*, 082902.
[48] T. Song, H. Tan, A. C. Robert, S. Estandia, J. Gázquez, F. Sánchez, I. Fina, *Appl. Mater. Today* **2022**, *29*, 101621.
[49] J. Barthel, *Ultramicroscopy* **2018**, *193*, 1.
[50] I. Fina, L. Fàbrega, E. Langenberg, X. Martí, F. Sánchez, M. Varela, J. Fontcuberta, *J. Appl. Phys.* **2011**, *109*, 074105.
[51] F. Liu, I. Fina, D. Gutiérrez, G. Radaelli, R. Bertacco, J. Fontcuberta, *Adv. Electron. Mater.* **2015**, *1*, 1500171.
[52] W. S. M. Werner, K. Glantschnig, C. Ambrosch-Draxl, *J. Phys. Chem. Ref. Data* **2009**, *38*, 1013.
[53] D. L. Windt, W. C. Cash, M. Scott, P. Arendt, B. Newnam, R. F. Fisher, A. B. Swartzlander, *Appl. Opt.* **1988**, *27*, 246.